

Evolution of PET technology – from early days, to the PennPET Explorer

Joel Karp, David Mankoff
Department of Radiology

P30 Didactics Lecture, April 6, 2020

Physics & Instrumentation Group

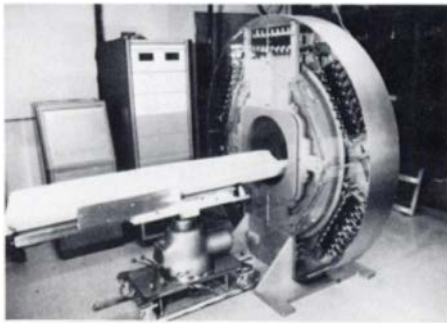
Department of Radiology, University of Pennsylvania



PET with multi-rings geometry (and septa)

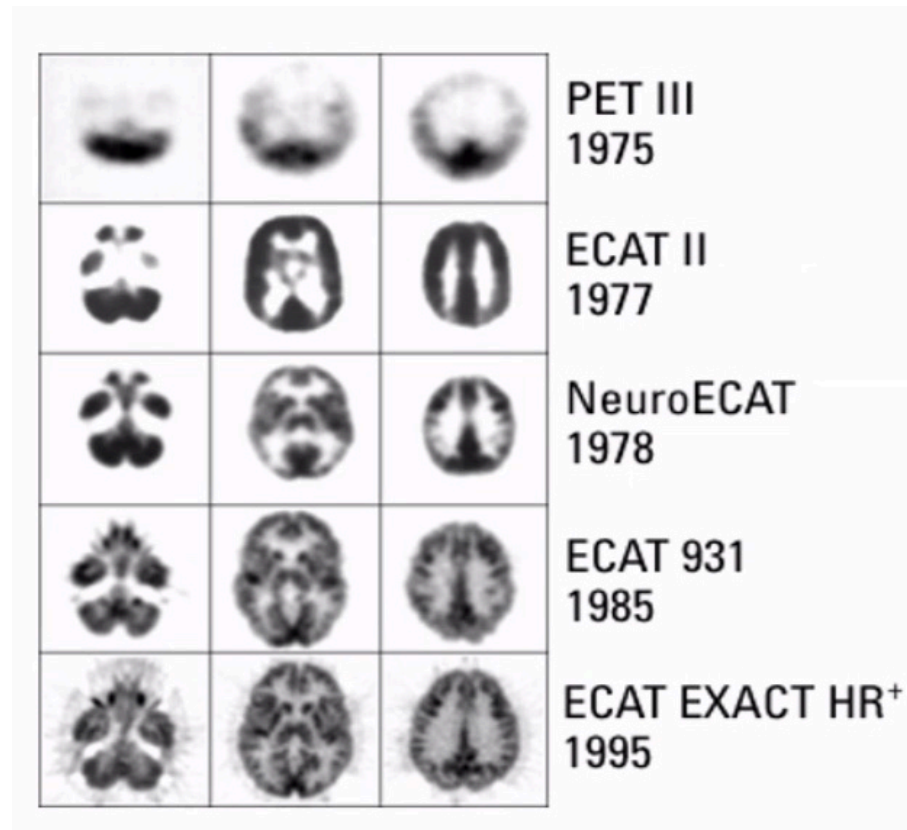
mid 1970's

Washington University
UCLA



mid 1908's

Casey, Nutt Block detector



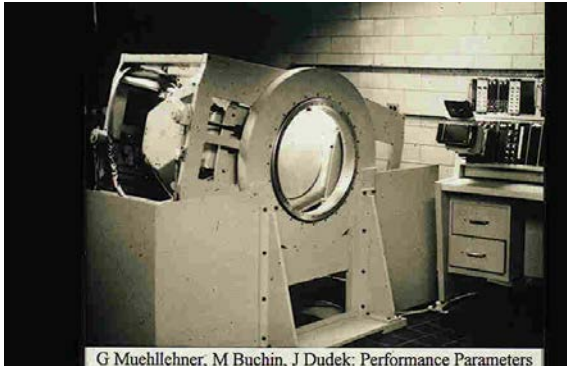
Higher spatial resolution with Anger-logic and multi-crystal BGO block

PET with Anger Cameras

University of Chicago 1975

2 Anger cameras in coincidence:

- Thick crystals
- No collimation
- Rotating



University of Pennsylvania 1998



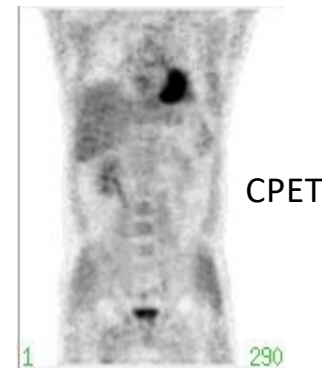
- 6 Curve-Plate detectors
- No Collimation – 3D
- Stationary



UGM Medical Systems
ADAC Laboratories C-PET

Iterative reconstruction – improved image quality
AC with ^{137}Cs singles Transmission scan – more accurate quantitation
Count-rate capability limited with NaI(Tl) – sufficient for FDG
Improved with pixelated detector with GSO – Allegro scanner

Higher sensitivity with 3D imaging acquisition and reconstruction



CPET

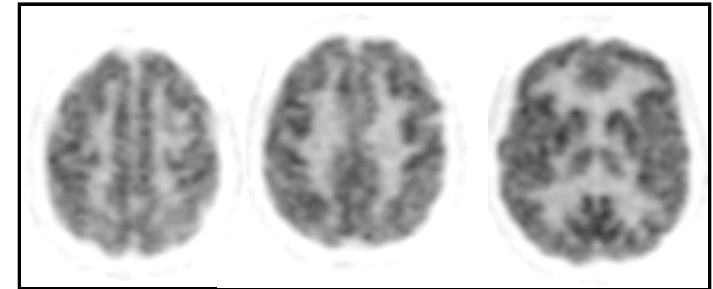
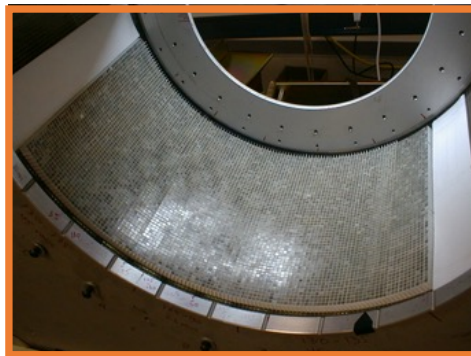


Allegro

Brain PET with Anger-logic Detectors



2001 G-PET Brain Scanner
Pixelated GSO detector

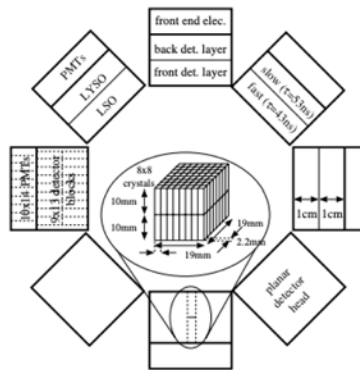


Spatial resolution ~ 3.7 mm
25.6 cm axial FOV

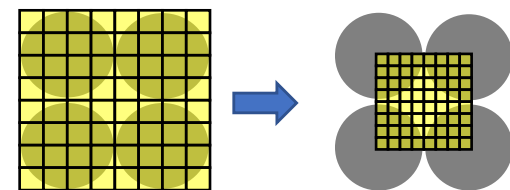
Siemens HRRT PET scanner



Spatial resolution ~ 2.7 mm



Dual-layer block detectors with smaller crystals and quadrant sharing arrangement of PMTs



Higher spatial resolution and sensitivity with dedicated brain PET

Also, improved quantification primarily due to a reduction in partial-volume effects (Van Helden *et al* (VUMC), JNM 2009).

TOF Positron Emission Tomography scanners

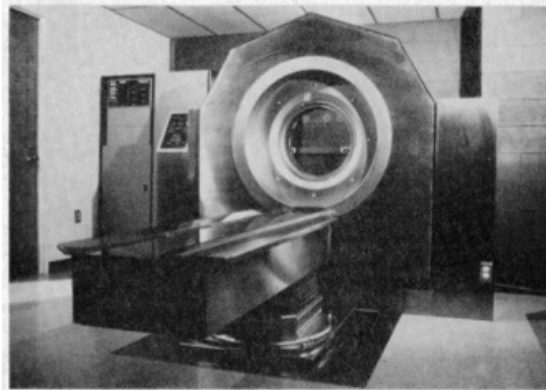
Washington University

CEA-LETI, Grenoble, France

University of Texas

1979-1983

Super PETT 1



Ter-Pogossian et al, TMI 1982

1-to-1 coupling
(25 mm ϕ x 45 mm : 28 mm ϕ PMT)

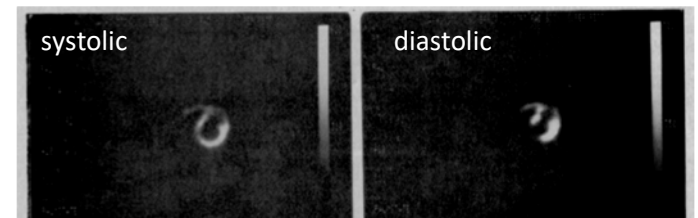
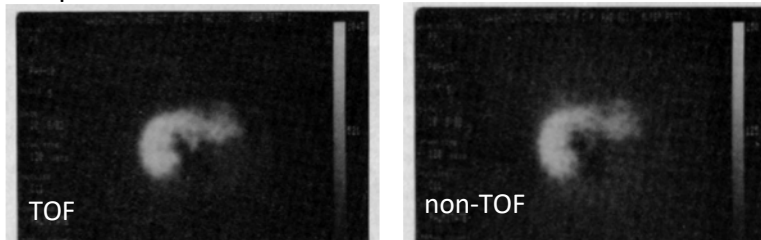


4 rings x 96 detectors CsF

$\Delta t = 500$ ps

Imaging with short-lived isotopes – ^{11}C , ^{15}O , ^{13}N

^{11}C -palmitate



Retrospective gating from list data

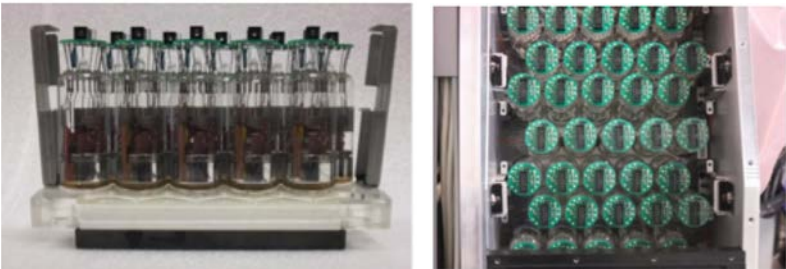
Higher count-rate imaging and TOF-assisted reconstruction with fast timing detectors

Modern PET-CT with 3D TOF

- LSO/LYSO - high light output enabled extension of block design *and* pixelated Anger-logic detector
- stopping power enabled high sensitivity, along with 3D imaging
- fast rise/decay of scintillation enabled precise timing for TOF

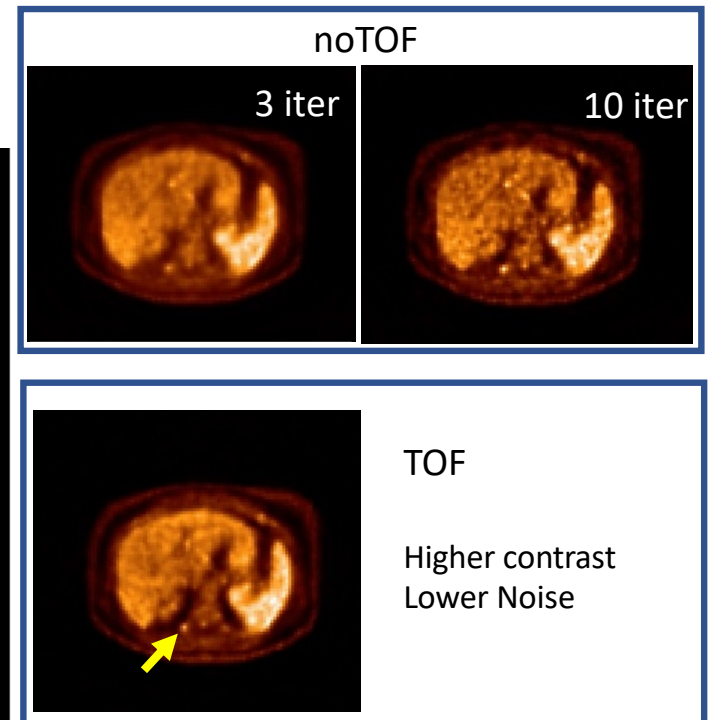
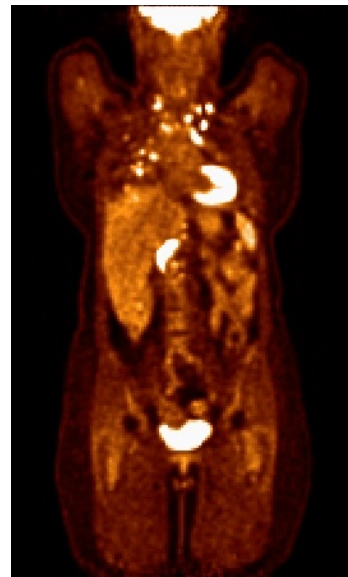


Philips Gemini TF



Anger-logic pixelated detector
– high spatial resolution and TOF

Fully 3D TOF PET-CT



Improved lesion detectability and quantitative accuracy for clinical FDG imaging with TOF

Commercial TOF PET/CT – all vendors

TOF 500-600 ps

2006

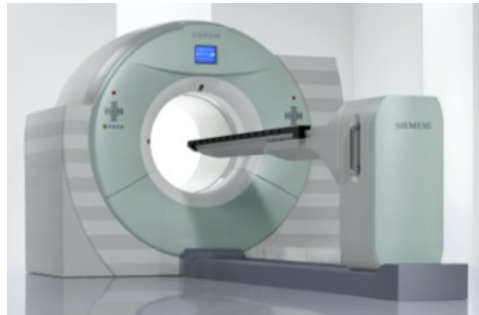


2010

Philips Gemini/Ingenuity TF



Siemens mCT



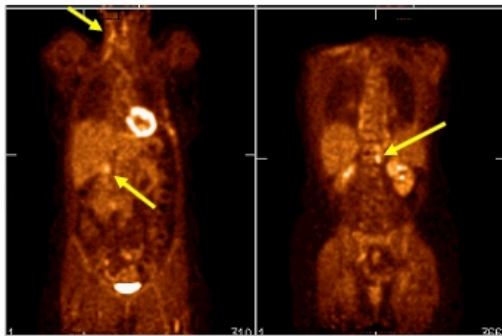
GE Discovery 690



8 min tot (1 min/bed)

**Light patient:
61 kg BMI = 22.2**

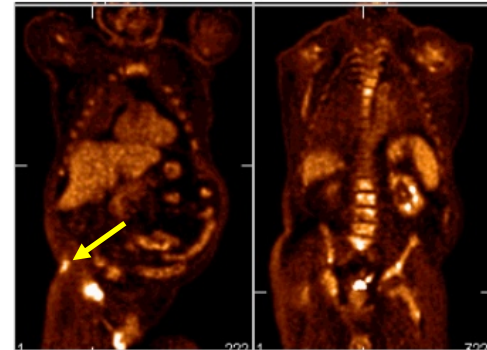
Head & neck cancer
- liver, spine lesions



27 min tot (3 min/bed)

**Heavy patient:
115 kg BMI = 38**

Abdominal
Cancer



Benefits of TOF lead to shorter scans (light patient) or improved image quality (heavy patients)

Images courtesy of Univ. Pennsylvania PET Center

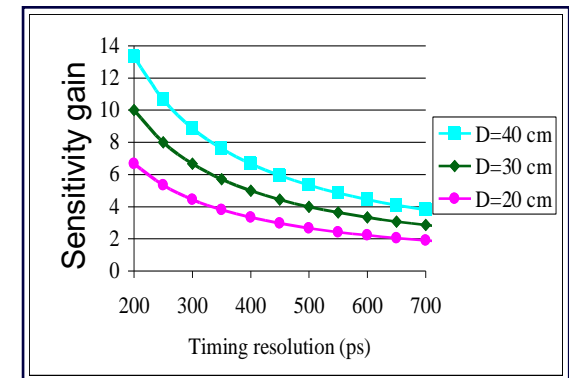
Improving Timing resolution

Benefits of TOF increase with better timing resolution

- Improved Signal-to-Noise
- Improved Quantitative Accuracy

Reduce statistical uncertainty or jitter in determining time stamp

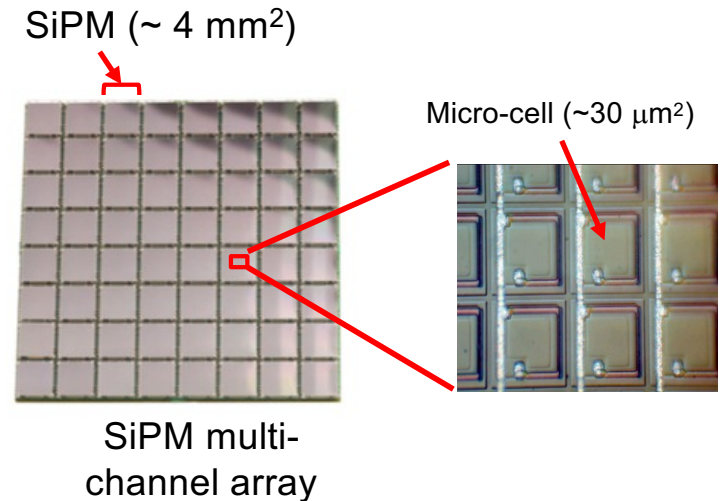
- New scintillators
 - Lanthanum Bromide
 - Ceramics (e.g., GluGAG)
 - LSO with optimized (e.g., Ca or Mg) dopants
- Improved detector designs
 - Dual-sided read-out
 - Thin layers of stacked detectors
 - Monolithic detectors – with depth-of-interaction
- New photo-sensor technology
 - Multi-channel PMTs
 - **Silicon photo-multiplier**



$$\text{Gain in SNR} = (D/\Delta x)^{1/2}$$

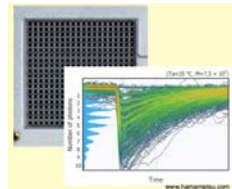
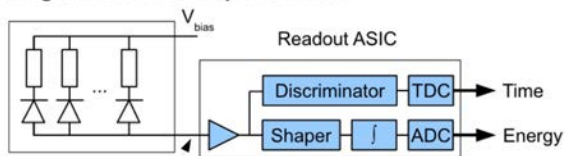
New Photo-sensor: Si-PMs

- Small APDs operating in Geiger mode with hundreds of micro cells per mm²:
 - Small, compact design
 - Can operate in MR
 - High gain, no need for amplification
 - Very high QE
 - Photo Detection Efficiency (PDE) = QE x Fill ~ 25-50%
 - Fast timing characteristics
 - Potential for low encoding (e.g. 1-to-1)
 - Multiple vendors
 - Hamamatsu, SensL, FBK/Broadcom, PDPC

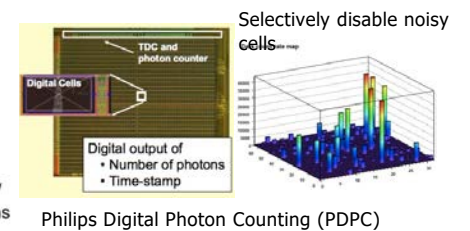
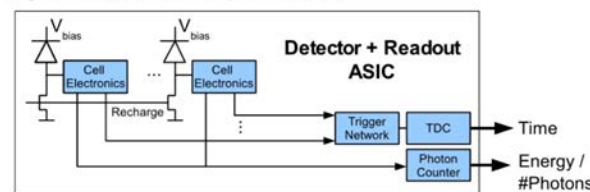


- Analog devices requires ASIC for signal processing Digital devices have electronics embedded on chip

Analog Silicon Photomultiplier Detector

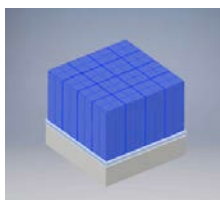
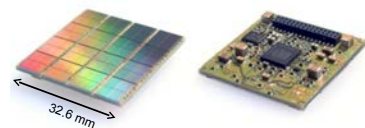


Digital Silicon Photomultiplier Detector



Philips Vereos

2012 pre-production, 2017 production



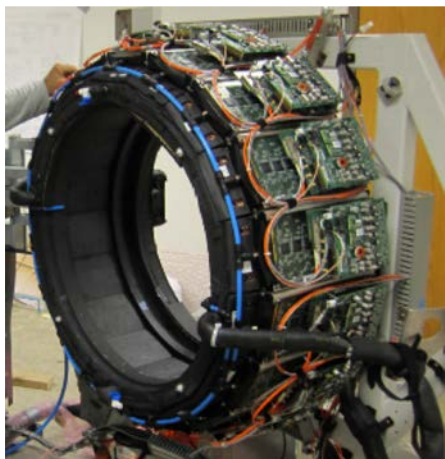
- 3.86 x 3.86 x 19 mm³ thick LYSO
- Axial FOV: 16.4 cm
- TOF: 320ps

Digital SiPM chip is a 8x8 channel device

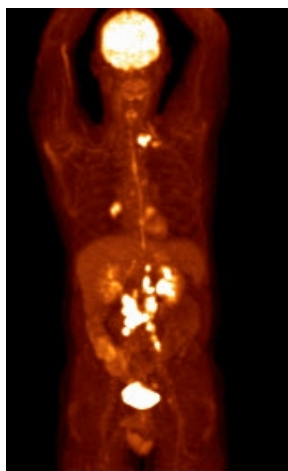
- 1 crystal per SiPM channel

MIP images for BMI=24 patient 13.4 mCi, 60 min p.i.

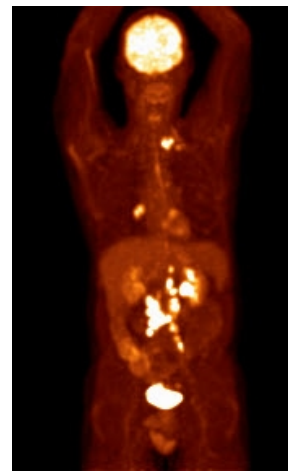
Courtesy, Drs. Michael Knopp, Jun Zhang, Ohio State Univ.



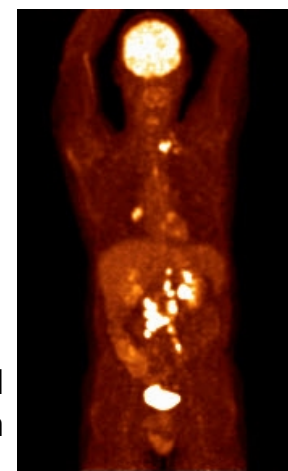
90s/bed
15min



30s/bed
5min



9s/bed
1.5min



High quality images in short scan time

Philips Vereos

Characterization of the Vereos Digital Photon Counting PET System

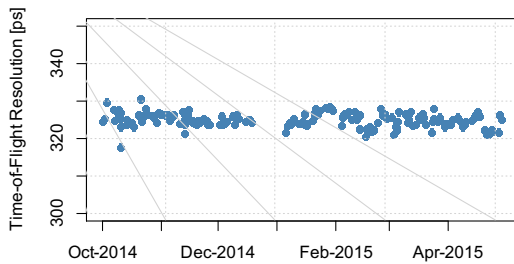
Miller et al, SNM 2015



THE OHIO STATE UNIVERSITY
WEXNER MEDICAL CENTER
Wright Center of Innovation in Biomedical Imaging

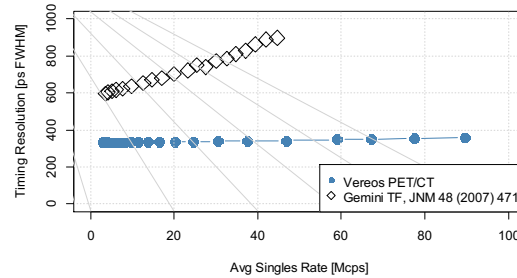
PHILIPS

TOF and count stability better than 1% over 7 months



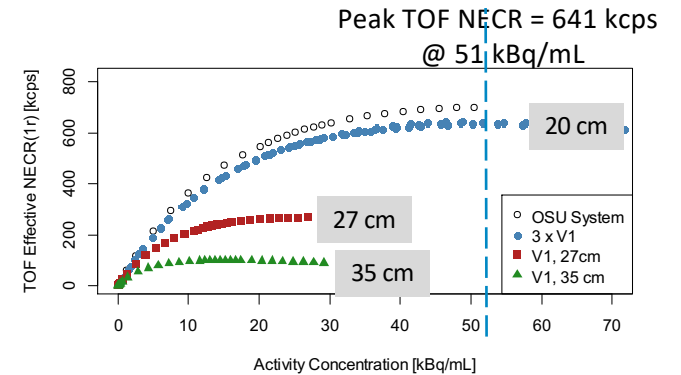
TOF Resolution Stability Over Time

TOF resolution stable within 5% up to peak NECR



TOF Resolution Stability Over Count Rate

First-class count rate performance



Spatial Res = 4.1 mm at center
5.1 mm at 20 cm

Siemens Biograph Vision

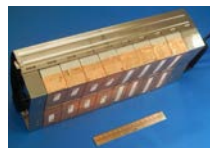
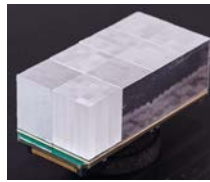
2018



- 3.2 x 3.2 x 20 mm³ thick LSO
- Axial FOV: 26.3 cm
- TOF: 215 ps

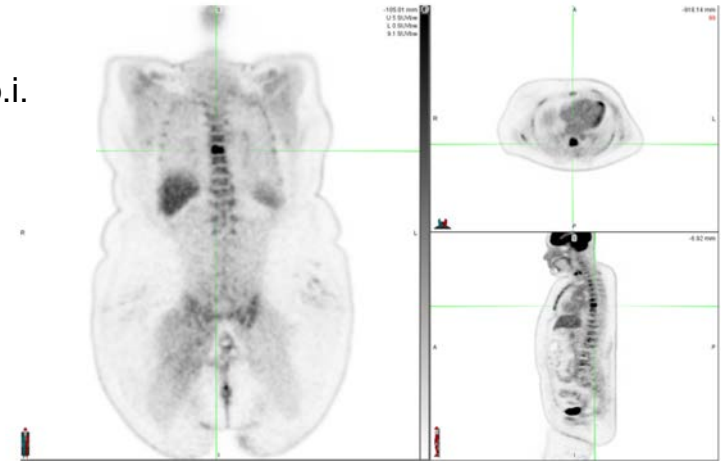
Mini-block, 5x5 array of crystals coupled to a SiPM chip with 4x4 array of channels

- ~ 1.5 crystals per SiPM channel



41 yo F with breast cancer
BMI 43.6

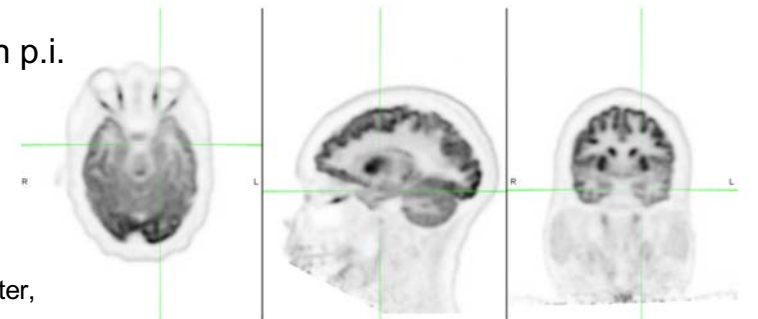
15 mCi FDG, 54 min p.i.
11 min scan
CBM @ 1.4 mm/s



Bony metastasis
in thoracic spine

27 yo F with drug resistant epilepsy

15 mCi FDG, 46 min p.i.
10 min scan

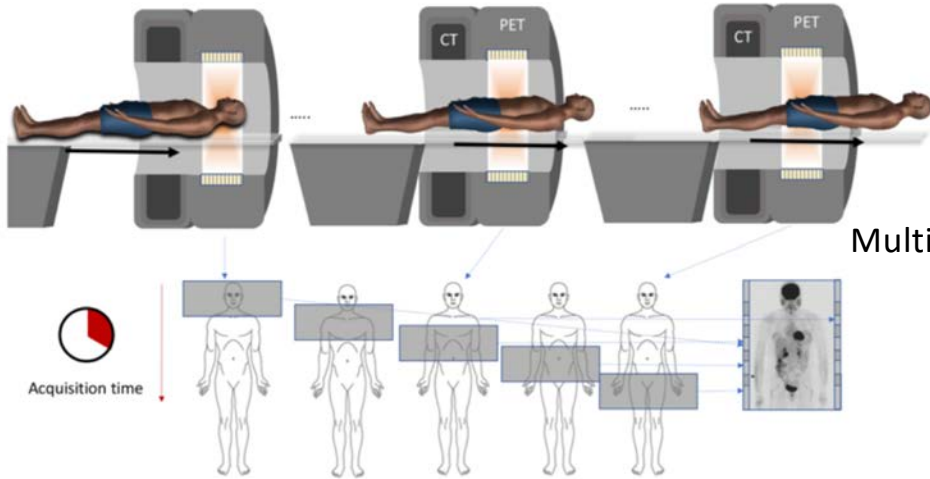


Decreased uptake consistent
with left-sided seizure onset

Images courtesy PET Center,
University of Pennsylvania

What is TB (Total-Body) PET?

Commercial PET-CT: Axial FOV 15-30 cm



Total-Body PET-CT: Axial FOV > 70 cm

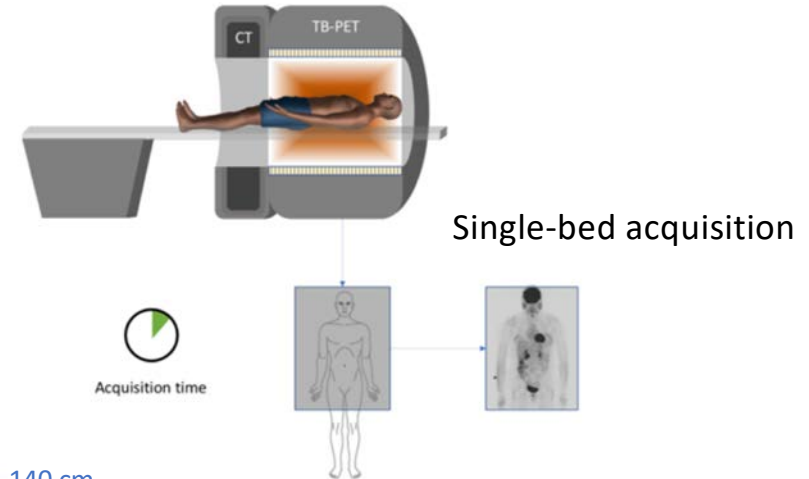
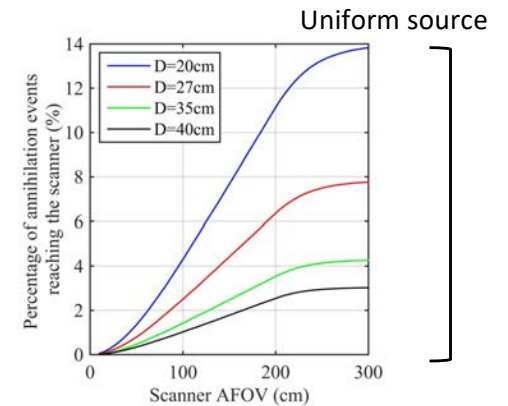
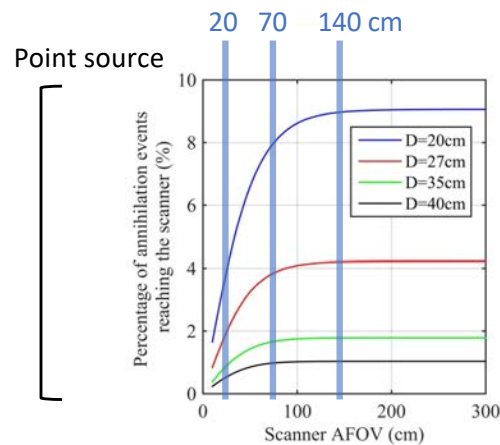


TABLE I
RELATIVE SENSITIVITY FOR SELECTED SCANNER AXIAL LENGTHS AS CALCULATED FOR THREE DIFFERENT IMAGING SETUPS. THE PHANTOMS ARE 200 CM LONG CYLINDERS.

Scanner AFOV (cm)	20	70	100	140	200
Point source in a 20 cm ϕ cyl.	1	2.4	2.7	2.8	2.8
Uniform source in a 20 cm ϕ cyl.	1	10	18	29	46
Uniform source in a 35 cm ϕ cyl.	1	14	24	38	58



Research and Translational Applications

- High sensitivity
 - Reduce dose or scan time
 - Delayed imaging to capture slow biology
- Simultaneous imaging of large volume
 - Bio-distribution of new radio-tracers
 - Dynamic imaging of multi-organ systems
 - brain-body
- Improved quantitative accuracy of kinetic modeling for biologic parameter calculation

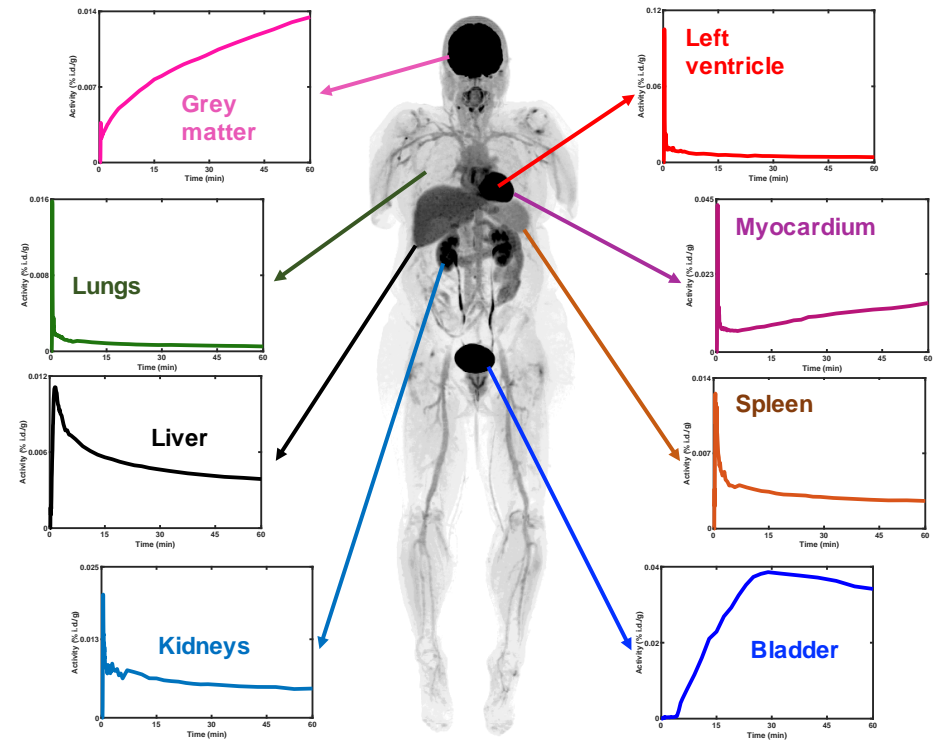


Image courtesy S. Cherry, UC Davis

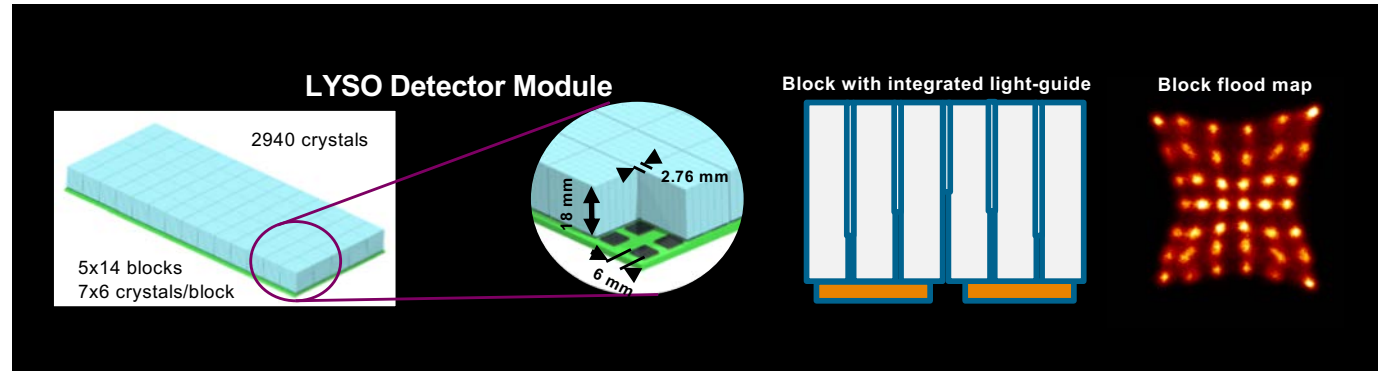
Long AFOV scanners: Anger logic vs. 1-to-1 coupling with SiPMs

uEXPLORER



194 cm AFOV

uEXPLORER PET Detectors: 10:1 encoding, crystals:SiPMs



- TOF = 505 ps, 3-mm spatial resolution

Courtesy, Hongdi Li, UIH America

PennPET Explorer



70-140 cm AFOV

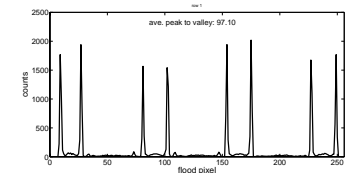
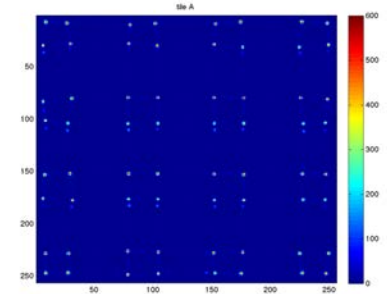
PennPET Detectors: 1:1 encoding, crystals:SiPMs



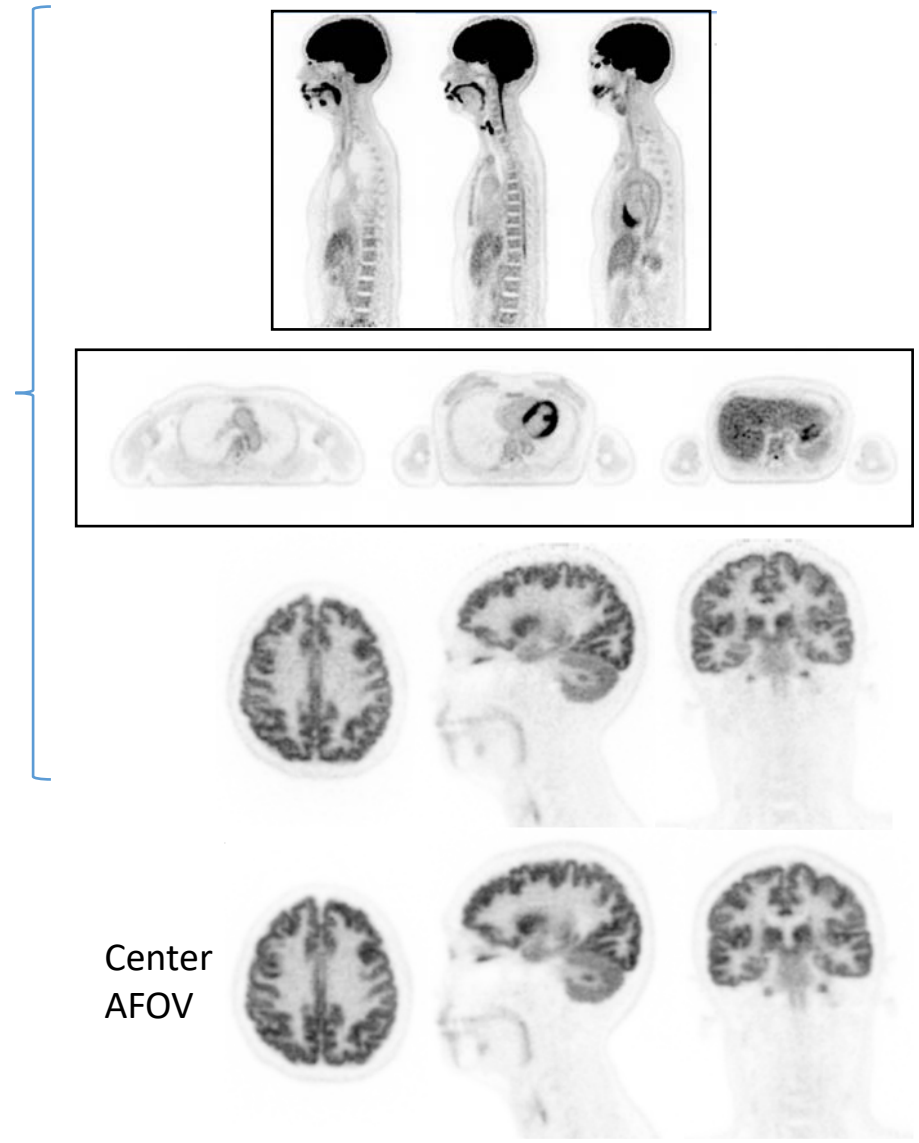
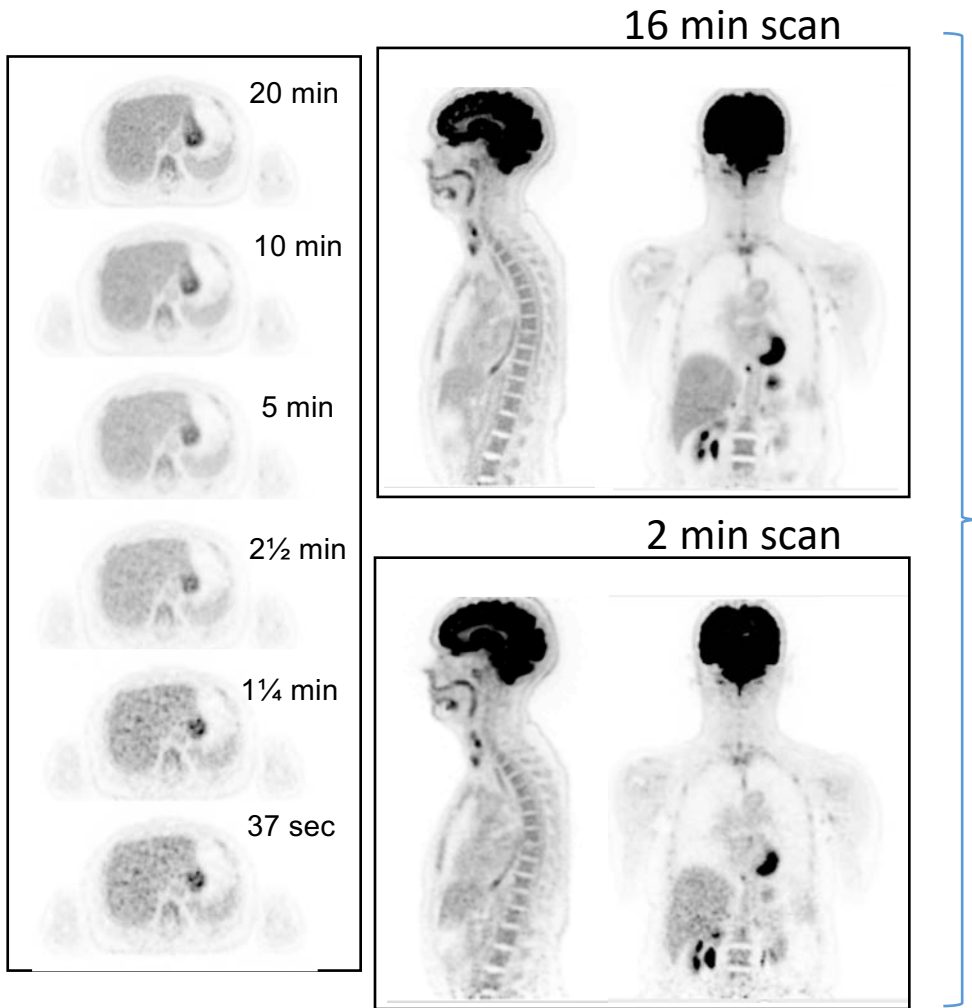
3.86 x 3.86 x 19 mm³ LYSO
PDPC digital SiPM

- TOF = 250 ps, 4-mm spatial resolution

2D flood



PennPET Explorer: Human studies

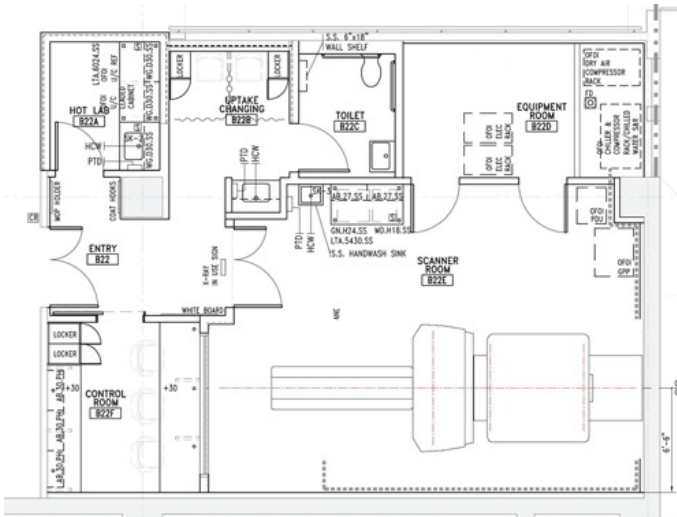
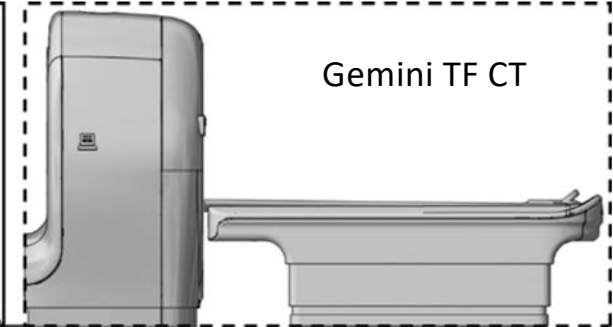
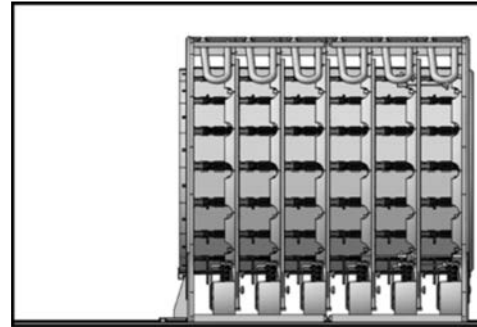


Scalable: 3 rings to 6 rings

3-ring PennPET Explorer



6-ring – 1.4 meter

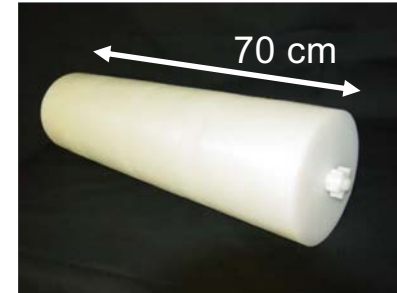


PennPET Explorer Imaging Facility -Stemmler B22



Summary

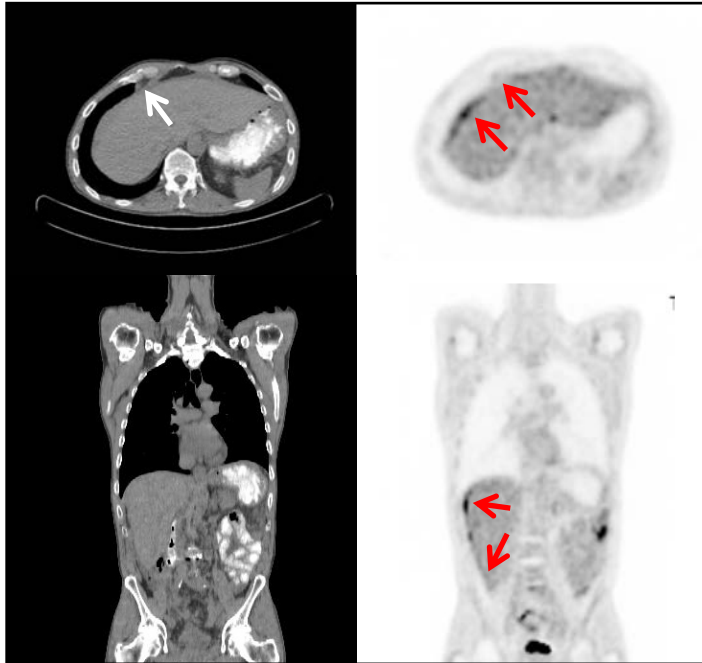
- Complete expansion to 6 rings
- Acceptance testing
 - Gemini TF CT completed
 - PET – will follow NEMA 2018
 - Designed for scanners with standard AFOV
 - Spatial resolution, sensitivity, count-rate capability, image quality
- Quantitative calibrations
 - ACR phantom – SUV cylinders, background
 - Routine QC – daily, monthly/quarterly, annual
- Resume human imaging – research IRB
 - Emphasize applications for whole-body PET



PennPET Explorer: Clinical studies

M 60 y.o, 173 cm, BMI 20.1
15 mCi FDG

Clinical PET/CT scan
1 hr p.i.



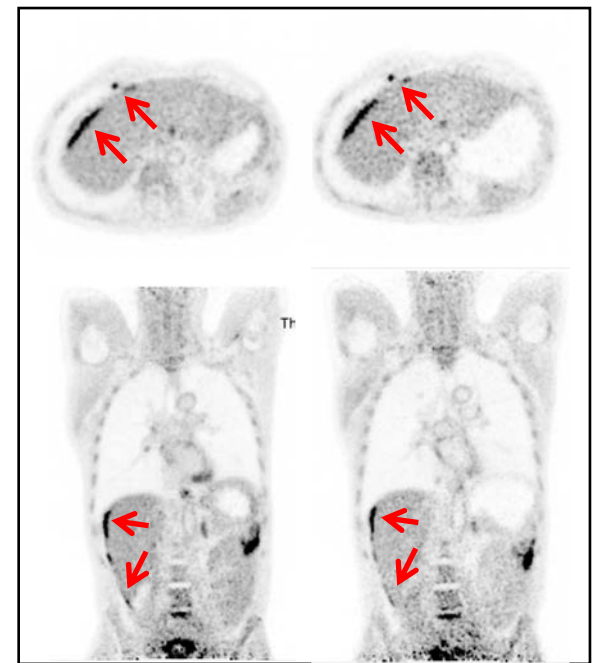
15 min scan

Disease of the
peritoneum



Improved clarity
of disease

PennPET scan
2.75 hr 4.25 hr (~ 1/4 dose)



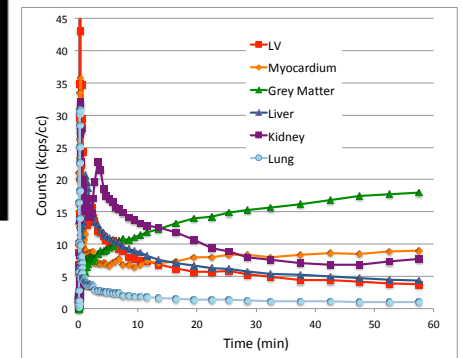
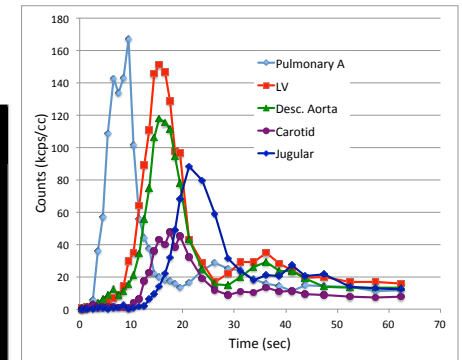
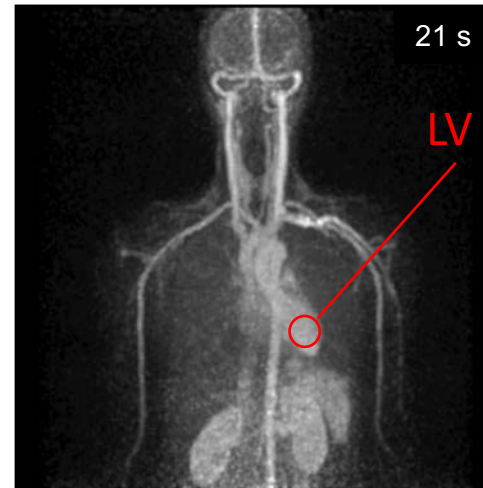
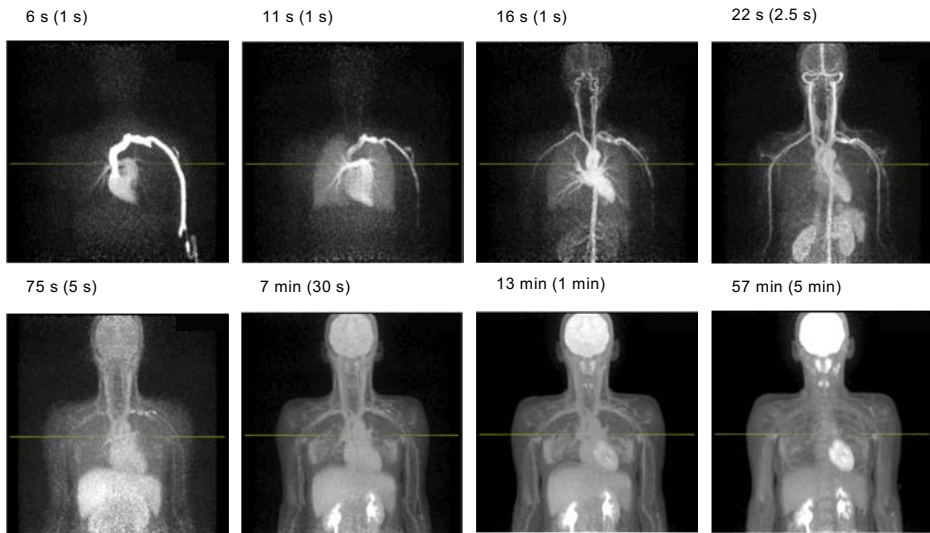
10 min scan

10 min scan

PennPET Explorer: Dynamic studies

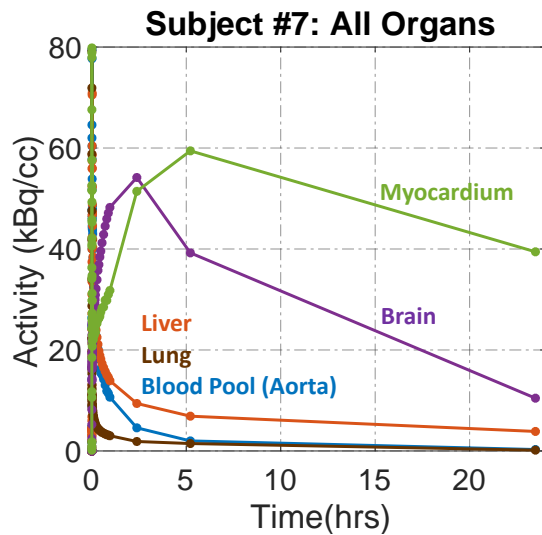
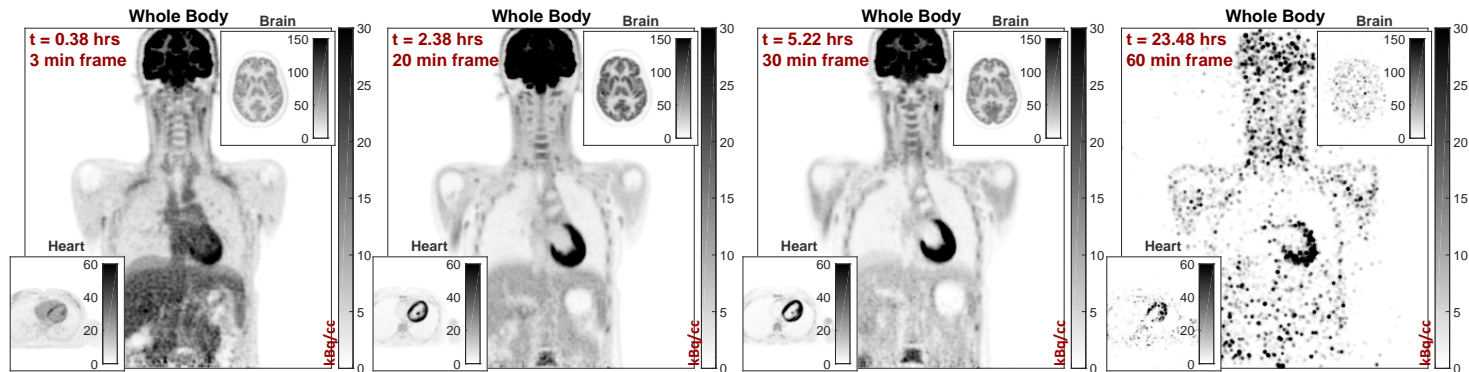
F 29 y.o, 177 cm, BMI 19.3

15 mCi FDG



Bolus injection: TACs of blood input function measured at several vessels over first minute after injection, and TACs of major organs over first hour after injection

PennPET Explorer: Delayed studies



- Activity in the brain decreases over time more quickly than in myocardium implying that G6Pase is activated to break down $[^{18}\text{F}]\text{FDG-6P}$

High Sensitivity enables the study of slow biological processes

Energy Metabolism & Biogenesis

FDG Measures Flux Through *Hexokinase*

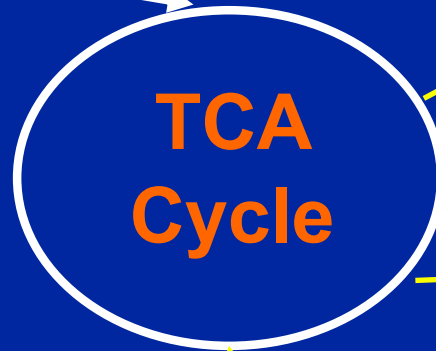
Glucose

Pyruvate

Ac-CoA

Glycolysis

Lactate



Energy and Biogenesis
Oxidative

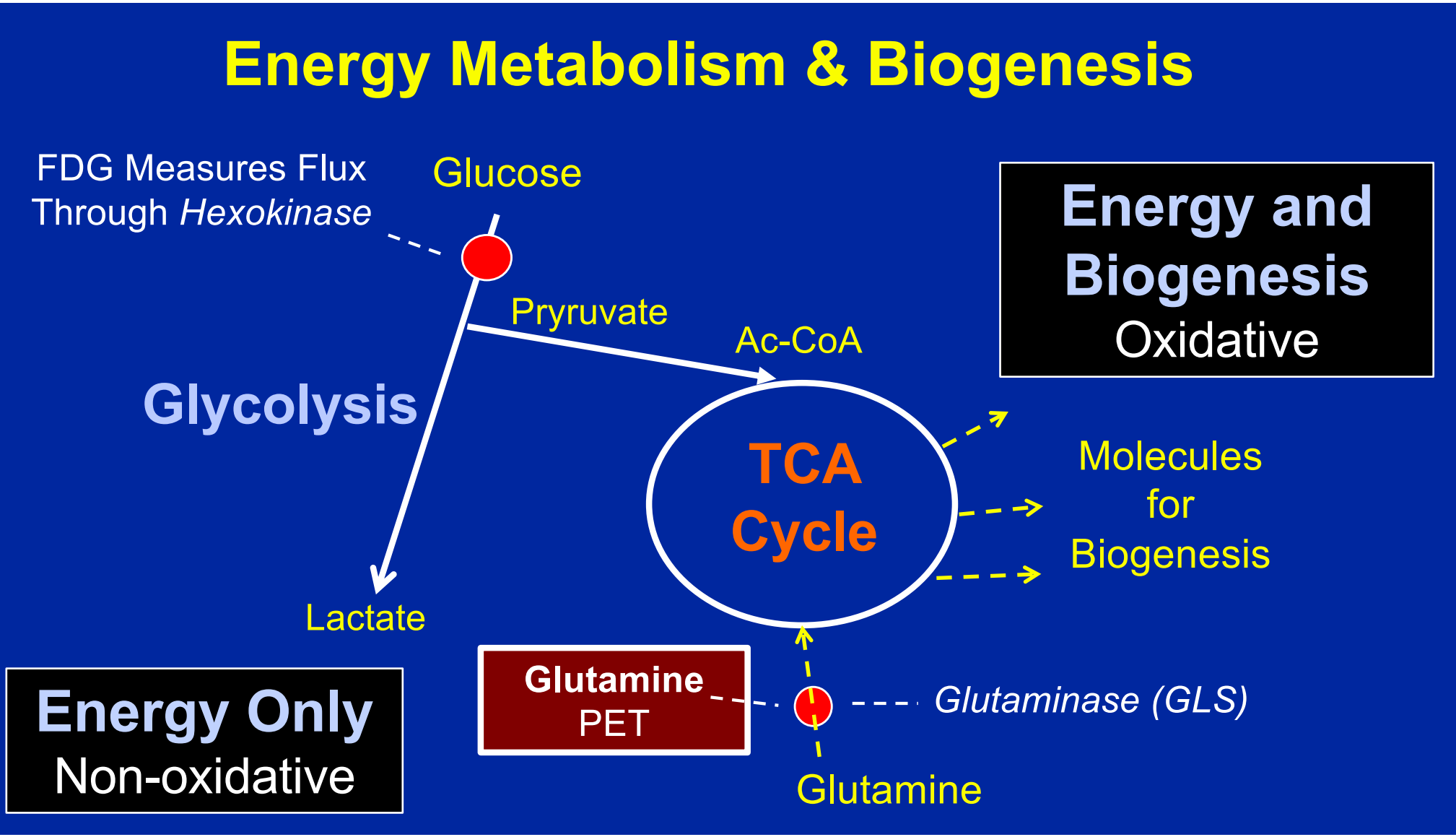
Molecules for Biogenesis

Energy Only
Non-oxidative

Glutamine
PET

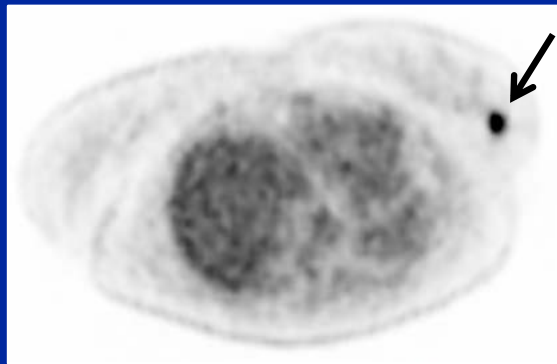
Glutamine

Glutaminase (GLS)

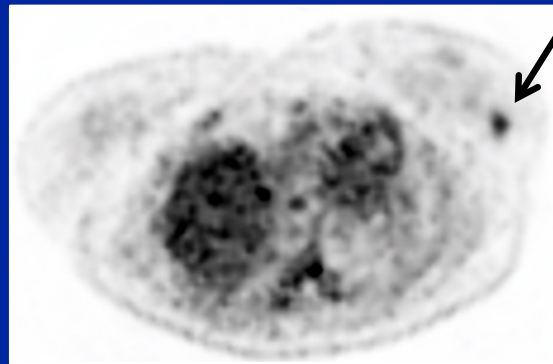


[¹⁸F]FDG and [¹⁸F]F-GLN PET/CT in Breast Cancer

[¹⁸F]FDG



[¹⁸F]F-GLN



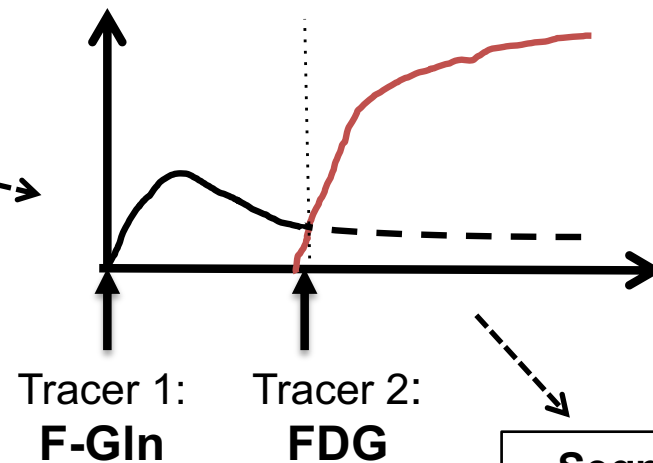
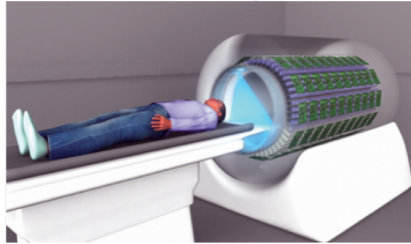
(Austin Pantel)



Total Body PET Enables Simultaneous Imaging of Glutamine and Glucose Metabolism

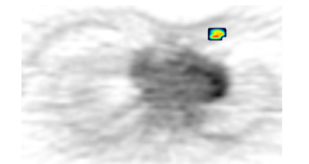
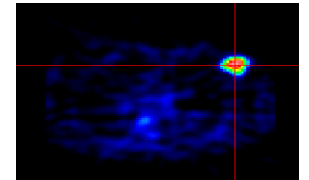
Mankoff, Karp, Kontos, O'Sullivan, Cancer Moonshot Grant R33-CA225310

Large-Volume
PET Tomograph



Segmentation
and Mixture
Analysis

Parametric
Images



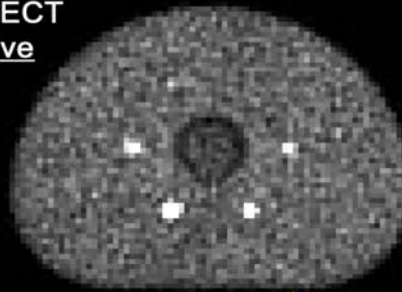
Metabolic
Heterogeneity

Dynamic data analysis with 4D reconstruction tools

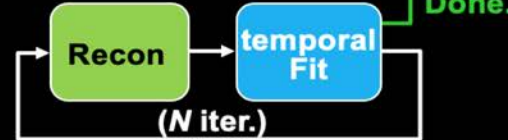
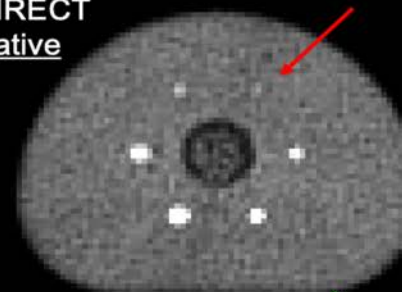
Matej & Gravel

4D vs conventional 3D DIRECT approaches

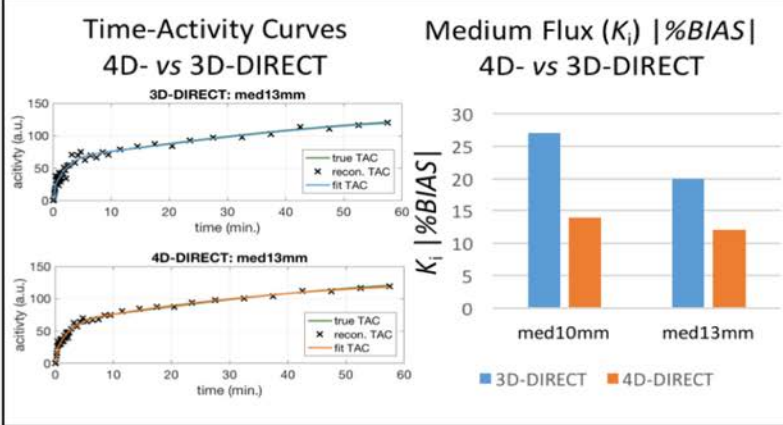
3D-DIRECT
iterative



4D-DIRECT
iterative



Frame 45 @ 55 min. p.i. (frame dur. = 5 min.)

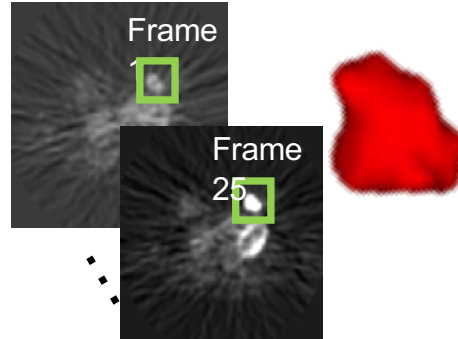


True, reconstructed and fit time-activity curves (left), with K_i absolute %BIAS (right) obtained from the iterative 4D-DIRECT reconstruction (orange) and from the iterative 3D-DIRECT reconstruction (blue) fitting methods at iteration 15, for the medium flux lesions of the dynamic IQ phantom.

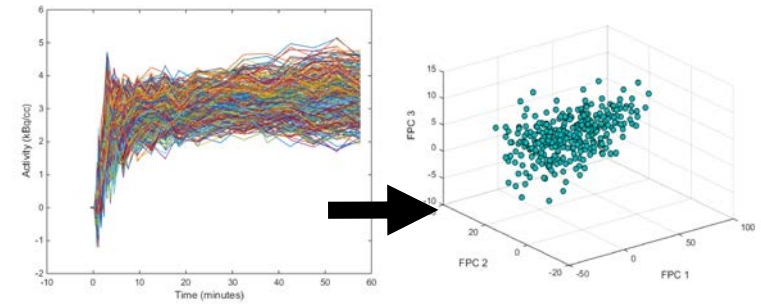
Contributors: Paul Gravel, Margaret Daube-Witherspoon, Joel Karp, Yusheng Li, David Mankoff, Varsha Viswanath, and Samuel Matej.
Funding: National Institutes of Health under Grants R33-CA225310 and R01-EB023274.

4D Imaging biomarkers of functional tumor heterogeneity (FTH)

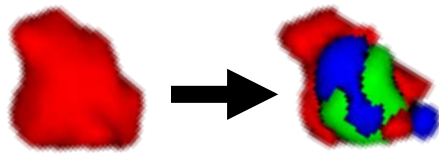
1. 3D tumor segmentation



2. Summarize TACs using functional principal components



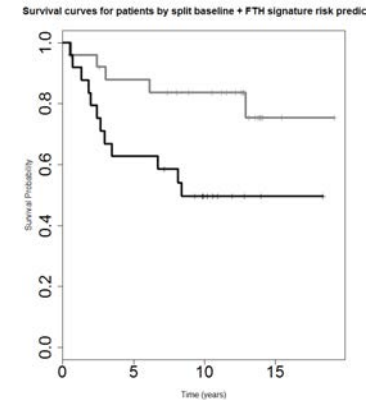
3. Segment tumors into 3 sub-regions using novel 4-D segmentation



4. Radiomic biomarker: FTH imaging signature



5. Recurrence free survival analysis



Spatial + Temporal = 4D functional tumor heterogeneity (FTH)

Chitalia and Kontos

Chitalia et al., *Radiomic Functional Intra-Tumor (Rad-FIT) clustering for characterizing functional tumor heterogeneity: Evaluation as a prognostic dynamic FDG-Pet biomarker for breast cancer*, in progress